

Electromechanical Coupling Characteristics Analysis and Research of Rotation-Parallel Flexible Robot Manipulator

zhi xiao (✉ hit_wz2021@163.com)

Zhejiang University of Technology

Wenhui Zhang

Nanjing Xiaozhuang University

Research Article

Keywords: Flexible operating manipulator, Electromechanical coupling, Vibration characteristics, Dynamic characteristics

Posted Date: January 11th, 2022

DOI: <https://doi.org/10.21203/rs.3.rs-1206532/v1>

License:   This work is licensed under a Creative Commons Attribution 4.0 International License.

[Read Full License](#)

Electromechanical Coupling Characteristics Analysis and Research of Rotation-Parallel Flexible Robot Manipulator

Wenhui Zhang^{1,4,5}, Zhi Wen^{1,2*}, Yangfan Ye³, Jinmiao Shen^{1,2}, Xiaoping Ye^{4,5}

1. School of Electromechanical Engineering, Nanjing Xiaozhuang University, Nanjing, China;

2. School of Machinery and Automatic Control ,Zhejiang Sci-Tech University, Hangzhou, China;

3.Zhejiang engineering geophysical survey and Design Institute Co., Ltd, Hangzhou, China;

4. Zhejiang Province Key Laboratory of Aerospace Metal Tube Forming Technology and Equipment, Lishui,China;

5. Key Laboratory of Digital Design and Intelligent Manufacturing for Creative Cultural Products of Zhejiang Province, Lishui ,China

Corresponding author: Zhi Wen (e-mail: hit_wz2021@ 163.com).

This work was supported by the National Natural Science Foundation of China (61772247), the natural science foundation of Zhejiang Province (LZ21F020003, LY20E050002), the open fund of Zhejiang Key Laboratory of Aerospace metal conduit plastic forming technology and equipment (zmxzh2021001), and the high-level training project of Nanjing Xiaozhuang University (2020 NXY14).

ABSTRACT RP(Rotation-Parallel) flexible robot as a typical electromechanical system. The complex electromechanical coupling effect in the system has a significant impact on the dynamic characteristics and stability of the flexible manipulator. This article investigates the electromechanical coupling dynamics and vibration response characteristics of flexible robot manipulator driven by AC(Alternating Current) servo motor with considering the start-up dynamic characteristics of the motor. Firstly, the physical model including the coupling of electromagnetic and mechanical system is established, and the dynamic model of the whole system is derived based on the global electromechanical coupling effect and Lagrange-Maxwell equations. Secondly, the virtual simulation platform is constructed with the help of MATLAB/Simulink, and the output speed characteristics of the motor drive end and the motion of the moving base are analyzed. Finally, through the joint simulation of MATLAB/Simulink dynamic simulation model and ADAMS/Controls virtual prototype model, the vibration characteristics of flexible manipulator under electromechanical coupling are obtained. The result demonstrates that the electromechanical coupling effect at the motor driving end has an obvious influence on the dynamic characteristics of the flexible manipulator, which is manifested in the increase of the vibration displacement amplitude of the flexible manipulator. With the increase of motor speed, the change of elastic vibration of flexible manipulator becomes larger, which shows that the electromechanical coupling effect of motor driving end has a greater impact on the dynamic characteristics of flexible manipulator at high speed. The analysis results are of great significance to improve the dynamic performance of motor-driven flexible robot manipulator.

INDEX TERMS Flexible operating manipulator; Electromechanical coupling; Vibration characteristics; Dynamic characteristics

I. INTRODUCTION

RP (Rotation Parallel) flexible robot system as a typical electromechanical coupling dynamic system, it is a complex electromechanical coupling relationship between the driving system and the actuator, which generates system excitation through the transmission system^[1-3]. As a high-speed and light structure, the system excitation caused by

electromechanical coupling effect will be more significant because of its low modal frequency. Therefore, the influence of electromechanical coupling effect in the system should be fully considered when analyzing the dynamic characteristics of flexible manipulator^[4].

Taking the permanent magnet AC servo drive motor system as an example, there are coupling factors in the whole system, such as the coupling between the electromagnetic parameters of the drive system and the mechanical parameters of the mechanical system, the coupling between the current harmonic in the armature circuit of the drive system and the transmission system, the coupling between the control parameters of the motor speed control system and the mechanical parameters of the servo system, and the coupling between the servo system and the load system^[5]. Lin Lihong et al.^[6] studied the precision transmission system and concluded that the output of the servo drive circuit has harmonic effect, and the output electromagnetic thrust of the motor has multi-order harmonic components, which is easy to excite the system vibration, and the excitation effect is generated through the action of the transmission system, thus affecting the dynamic characteristics of the system. By analyzing the electromechanical coupling characteristics of high-speed and high acceleration drive systems. Lu Bingheng et al.^[7] obtained that for high-speed light structures, the system excitation generated by coupling factors will be more prominent. Qiu Zhicheng et al.^[8,9] designed a device to simulate the space flexible manipulator, established the coupling dynamic model of the electrically driven flexible manipulator, and studied the influence of electromechanical coupling effect on the vibration characteristics of the flexible manipulator. Pratiher et al.^[10] studied the nonlinear vibration and stability of flexible robot with load under basic harmonic excitation. Qiu Jiajun^[11,12] analyzed the electromechanical coupling dynamic characteristics of mechanical system in detail, and proposed the theoretical analysis method of electromechanical dynamics to solve this kind of problem. Meng Jie et al.^[13] established the electromechanical coupling model of machine tool motor spindle and studied the relationship between current and motor spindle output speed characteristics under electromagnetic torque coupling. In addition, for electromechanical systems with multiple coupling relationships, Wang Allen et al.^[14] proposed the basic idea of global coupling analysis and parallel partial coupling analysis for the multiple coupling of electromechanical parameters and electrical parameters of modern large-scale complex electromechanical systems. Subudhi^[15] established the coupling dynamic model of multi flexible link flexible hinge manipulator based on hypothetical modal method and

Lagrange equation. According to the characteristics of electromechanical dynamics, Tang Huaping^[16] proposed a global modeling method of complex electromechanical system based on constraint function recursive group aggregation. Felix et al.^[17] studied the change of coupling effect between mechanical structure parameters and electrical parameters with the increase of motor torque. Meanwhile, Dwivedy et al.^[18] studied the nonlinear dynamics of the flexible arm with basic linear motion, and discussed the stability of the system under the conditions of considering the main parametric resonance, combine parametric resonance and internal resonance. Ju Jinyong studied the dynamic characteristics and nonlinearity of the system driven by high-power permanent magnet^[19]. At the same time, he also studied the electromechanical coupling vibration characteristics of the translational manipulator driven by AC servo motor^[20]. Liu et al.^[21] constructed the coupling dynamic model of motor drive system and analyzed its vibration response characteristics. Zhang Wei et al.^[22-25] studied the dynamic characteristics of thin plate structure under parametric excitation and external excitation. Wei^[26] studied the dynamic characteristics of flexible beam plate structure under fixed axis rotation and parametric excitation. However, at present, most studies consider the flexible manipulator alone, do not specifically consider the coupling relationship between the driving system and the actuator, and assume that the motion of the moving base connecting the flexible manipulator is uniform and constant. Therefore, in some fields with high precision requirements, the motion fluctuation generated by the system will produce some errors in the vibration characteristic analysis and vibration control of the flexible manipulator^[27,28].

In order to explore the influence of electromechanical coupling factors on the vibration characteristics of flexible manipulator, firstly, the electromechanical coupling dynamic physical model of mobile flexible manipulator driven by permanent magnet servo system is established, and the experimental platform is built. Based on the electromechanical dynamic analysis method and combined with the physical parameters of the test object, the global electromechanical coupling dynamic equation of the system is deduced, the output speed characteristics of the motor driving end and the motion characteristics of the moving base are analyzed, and the vibration law of the flexible manipulator under electromechanical coupling is revealed.

Through the joint simulation of system dynamics simulation model and virtual prototype model, the vibration characteristics of flexible manipulator under electromechanical coupling are obtained, which provides a theoretical basis for the study of parametric vibration characteristics and elastic vibration control design of flexible manipulator.

II. Electromechanical Coupling Dynamics Analysis of Flexible Manipulator System

Since the invention of permanent magnet generator and motor in the 18th century, electromechanical coupling in mechanical system has become the object of research and analysis^[29,30]. As a typical complex electromechanical system, there are main coupling factors in the whole system, such as the coupling of electromagnetic parameters and mechanical parameters of the driving system, the coupling of current harmonics in the armature circuit and the transmission system, and the coupling of servo system and load system^[31-33]. The output of the driving circuit has harmonic effect, and the output electromagnetic thrust of the motor has multi-order harmonic components, which is easy to excite the system to produce vibration, and then affect the dynamic characteristics of the flexible manipulator through the action of the transmission system^[34,35]. In recently years, with the rapid development of flexible robot, the research on the dynamic characteristics of flexible manipulator has attracted the attention of many scholars. In the existing research on the dynamic modeling and dynamic characteristics of the flexible manipulator, the flexible manipulator is usually studied separately without considering the coupling effect between the driving system and the actuator, and it is assumed that the moving base connecting the flexible arm is constant in motion, without considering the motion fluctuation caused by electromechanical coupling. Therefore, in order to truly reflect the dynamic characteristics of the flexible manipulator in the system, the influence of electromechanical coupling effect of the system should be fully considered in the process of studying the vibration characteristics of the flexible manipulator^[36].

Based on the existing industrial RP flexible robot, the structural diagram as shown in Fig.1.

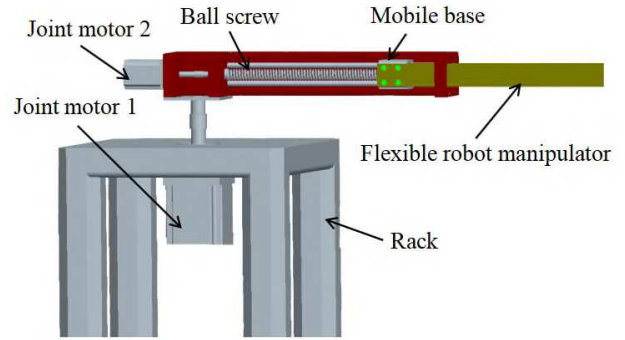


Figure 1 The structural diagram of RP flexible robot system

It can be seen from the above figure that the flexible robot system includes frame, driving system, roller lead screw, rigid moving base and flexible operating arm. The driving motor 1 can realize the rotary movement of the mechanical structure, the driving motor 2 can realize the translational movement of the roller lead screw, the flexible operating arm is connected with the rigid moving base through bolts, and then the actuator at the end of the operating arm can complete the corresponding operation tasks. Further, according to the law of energy conservation, the energy that drives the whole system of the flexible manipulator comes from electric energy, and the mechanical torque of the mechanical part should be equal to the electromagnetic torque of the permanent magnet synchronous drive motor, so the flexible manipulator system is constructed into a global electromechanical coupling diagram as shown in Fig. 2.

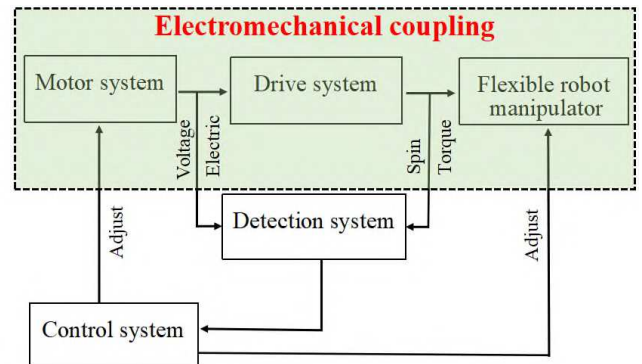


Figure 2 Global electromechanical coupling diagram

It can be seen from the above figure that the mechanical system, transmission system and execution system are connected through the mutual coupling of electric field and magnetic field. It completes the conversion from electrical signals such as voltage and current to force and torque. It is a typical electromechanical coupling system.

1. Physical Model of System Structure

RP flexible robot system is a complex mechanical structure including drive system, transmission system and execution system. The driving system mainly selects permanent magnet AC servo motor, which is composed of stator and rotor. When the stator is connected with three-phase sinusoidal ac, the stator generates a space uniform rotating magnetic field. The stator magnetic field interacts with the rotor magnetic field to generate driving torque, driving the rotor rotation, so as to realize the conversion of electrical energy into mechanical energy. The driving system is composed of roller screw pair, moving guide rail pair and positioning base. The system selects a flexible manipulator. The permanent magnet AC servo motor is connected with the input end of the roller screw through the coupling, and the electric energy is converted into kinetic energy through the rotation of the rotor in the magnetic field, and then drives the moving slider on the roller screw to move, and finally realizes the action of the flexible operation arm. According to the working principle, the drive system, transmission system and execution system are simplified into the physical model shown in Fig.3.

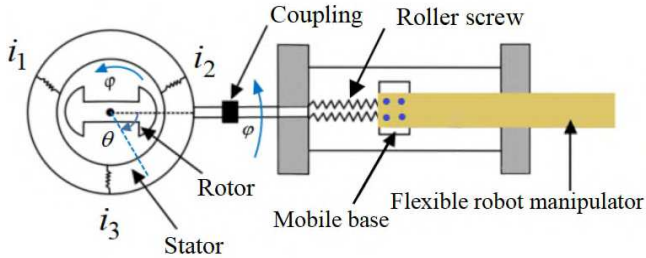


Figure 3 Global system physical model

2. Electromechanical Coupling Dynamic Equation

According to the above established system physical model, based on the electromechanical analysis dynamics method, the electromechanical coupling dynamics model among the driving system, transmission system and execution system of RP flexible robot is established by using Lagrange-Maxwell equation, and the coupling relationship between the output characteristics of synchronous motor and the motion characteristics of positioning base is analyzed according to this model. During the modeling process, the following assumptions are made for the driving motor and the flexible operating arm:

- 1) Ignore core saturation and eddy current loss.

- 2) The mutual inductance and self inductance of each phase winding are constant, and the air gap is evenly distributed.

- 3) The rotor has no damping winding and the permanent magnet has no damping effect.

- 4) The flexible manipulator satisfies the Euler-Bernoulli beam theory.

Firstly, the Lagrange-Maxwell operator can be expressed as:

$$L = T + W - U \quad (1)$$

Where, T represents the sum of the kinetic energy of the drive, transmission and execution system, W represents the magnetic field energy in the system, and U represents the elastic potential energy in the system.³

Secondly, the Lagrange-Maxwell equation can be expressed as:

$$\frac{d}{dt} \left(\frac{\partial L}{\partial \dot{e}_i} \right) - \frac{\partial L}{\partial e_i} + \frac{\partial E_r}{\partial \dot{e}_i} = Q_i \quad (2)$$

Where, E_r represents the dissipation function of the system and Q_i represents the non-conservative generalized force of the system.

(1) The kinetic energy of the whole mechanical system includes: the rotational kinetic energy of the driving motor, the rotational kinetic energy of the lead screw, the kinetic energy of the moving slider and the kinetic energy of the flexible operating arm, so the sum of the kinetic energy of the system is:

$$T = \frac{1}{2} \left[J_s \left(\frac{d\theta}{dt} \right)^2 + J_b \left(\frac{d\theta}{dt} \right)^2 + \frac{1}{4} m_s D^2 \left(\frac{d\theta}{dt} \right)^2 + \int_0^L \rho S \left(\frac{D}{2} \cdot \frac{d\theta}{dt} + \frac{\partial w}{\partial t} \right)^2 dx \right] \quad (3)$$

Among them, the first item represents the rotational kinetic energy of the driving motor; the second item represents the rotational kinetic energy of the roller lead screw; the third item represents the kinetic energy of the moving slider and the fourth item represents the kinetic energy of the flexible operating arm. In this analysis system, the end mass is ignored. J_s is the moment of inertia of the motor, J_b is the moment of inertia of the roller lead screw, m_s is the mass of the moving slider, θ is the rotation angle of the motor, ρ is the density of the flexible operating arm, S is the cross-sectional area of the flexible operating arm and D is the diameter of the roller lead screw.

(2) The magnetic field energy in the system includes: the magnetic energy generated W_1 by the stator current in the AC permanent magnet synchronous motor; the magnetic energy generated W_2 by the rotor permanent magnet and the magnetic energy generated W_3 by the interaction between the rotor flux and the stator current. Due to the difference between the three-phase currents 120° and the relatively large number of slots between each pole, it can be considered that the magnetic energy generated by the air gap of the rotor permanent magnet W_2 does not change with the rotation of the rotor, that is $W_2 = c$ (c is a constant). Therefore, the sum of magnetic energy in the system is:

$$\begin{aligned}
W &= W_1 + W_2 + W_3 \\
&= \frac{1}{2}L_1i_1^2 + \frac{1}{2}L_2i_2^2 + \frac{1}{2}L_3i_3^2 + \\
&\quad H_n i_1 i_2 + H_n i_1 i_3 + H_n i_2 i_3 + c \\
&\quad + i_1 \psi_f \cos \theta + i_2 \psi_f \cos(\theta - \frac{2}{3}\pi) + \\
&\quad i_3 \psi_f \cos(\theta + \frac{2}{3}\pi) \quad (4)
\end{aligned}$$

Where, L_1 、 L_2 、 L_3 respectively represent the self-inductance of three-phase stator winding; H_n represent the mutual inductance of three-phase stator winding, i_1 、 i_2 and i_3 represent the three-phase current of motor.

(3) The potential energy in the system mainly includes the elastic potential energy when the roller lead screw is twisted and the elastic potential energy of the flexible operating arm. Therefore, the sum of potential energy in the system is:

$$\begin{aligned}
U &= U_1 + U_2 \\
&= \frac{1}{2}K_b(\theta - \frac{2\pi S}{p})^2 + \frac{1}{2}EI \int_0^l (\frac{\partial^2 \omega}{\partial x^2})^2 dx \quad (5)
\end{aligned}$$

Where, K_b represents the torsional stiffness of the roller lead screw, and EI represents the elastic stiffness of the flexible operating arm.

By introducing equations (3), (4) and (5) into equation (1), the Lagrange operator of the system can be obtained:

$$L = T + W - U$$

$$\begin{aligned}
&= \frac{1}{2} \left[J_s \left(\frac{d\theta}{dt} \right)^2 + J_b \left(\frac{d\theta}{dt} \right)^2 + \frac{1}{4} m_s D^2 \frac{\pi}{p} \left(\frac{dS}{dt} \right)^2 + \right. \\
&\quad \left. m_b \left(\frac{dS}{dt} \right)^2 + \int_0^l \rho S \left(\frac{D}{2} + \frac{\partial w}{\partial t} \right)^2 dx \right] \\
&\quad + \frac{1}{2} L_1 i_1^2 + \frac{1}{2} L_2 i_2^2 + \frac{1}{2} L_3 i_3^2 \\
&\quad + H_n i_1 i_2 + H_n i_1 i_3 + H_n i_2 i_3 \\
&\quad + i_1 \psi_f \cos \theta + i_2 \psi_f \cos(\theta - \frac{2}{3}\pi) \\
&\quad + i_3 \psi_f \cos(\theta + \frac{2}{3}\pi) \\
&\quad - \frac{1}{2} K_b \left(\theta - \frac{2\pi S}{p} \right)^2 - \frac{1}{2} EI \int_0^l \left(\frac{\partial^2 w}{\partial x^2} \right)^2 dx \quad (6)
\end{aligned}$$

(4) The dissipation function in the system mainly includes: resistance dissipation E_{r1} , electric rotor dissipation E_{r2} , friction dissipation E_{r3} between moving slider and roller lead screw.

$$\begin{aligned}
E_r &= E_{r1} + E_{r2} + E_{r3} \\
&= \frac{1}{2} R_1 i_1^2 + \frac{1}{2} R_2 i_2^2 + \frac{1}{2} R_3 i_3^2 + \frac{1}{2} R_b \left(\frac{d\theta}{dt} \right)^2 \\
&\quad + \frac{1}{2} R_f \left(\frac{dS}{dt} \right)^2 \\
&= \frac{1}{2} \left[R_1 i_1^2 + R_2 i_2^2 + R_3 i_3^2 + R_b \left(\frac{d\theta}{dt} \right)^2 \right. \\
&\quad \left. + R_f \left(\frac{dS}{dt} \right)^2 \right] \quad (7)
\end{aligned}$$

Where, R_1 、 R_2 and R_3 respectively represent the resistance of three-phase motor, R_b represents the resistance value of rotor and R_f represents the friction coefficient between sliding block and lead screw.

Bring equations (3), (4), (5) and (7) into equation (1) to obtain the Lagrange equation of the system:

$$\left[\begin{aligned}
\frac{\partial L}{\partial e_i} &= 0 \\
\frac{\partial L}{\partial i_1} &= L_1 i_1 + H_n i_2 + H_n i_3 + \psi_f \cos \theta \\
\frac{d}{dt} \left(\frac{\partial L}{\partial \dot{i}_1} \right) &= L_1 \left(\frac{di_1}{dt} \right) + H_n \left(\frac{di_2}{dt} \right) + H_n \left(\frac{di_3}{dt} \right) \\
&\quad - \frac{d\theta}{dt} \psi_f \sin \theta \\
\frac{\partial E_r}{\partial i_1} &= R_1 i_1
\end{aligned} \right. \quad (8)$$

By introducing the above formula into equation (2), the voltage equation of stator winding 1 can be obtained:

$$\begin{aligned}
u_1 &= L_1 \frac{di_1}{dt} + H_n \left(\frac{di_2}{dt} \right) + H_n \left(\frac{di_3}{dt} \right) \\
&\quad - \frac{d\theta}{dt} \psi_f \sin \theta + R_1 i_1
\end{aligned} \quad (9)$$

Similarly, the voltage equations of stator winding 2 and stator winding 3 can be obtained as follows:

$$\begin{aligned}
u_2 &= L_2 \frac{di_2}{dt} + H_n \left(\frac{di_1}{dt} \right) + H_n \left(\frac{di_3}{dt} \right) \\
&\quad - \frac{d\theta}{dt} \psi_f \sin \left(\theta - \frac{2}{3} \pi \right) + R_2 i_2
\end{aligned} \quad (10)$$

$$\begin{aligned}
u_3 &= L_3 \frac{di_3}{dt} + H_n \left(\frac{di_1}{dt} \right) + H_n \left(\frac{di_2}{dt} \right) \\
&\quad - \frac{d\theta}{dt} \psi_f \sin \left(\theta + \frac{2}{3} \pi \right) + R_3 i_3
\end{aligned} \quad (11)$$

When the output angle of the motor θ is taken as the research object in generalized coordinates, the vibration displacement equation of the flexible manipulator can be obtained.

According to equation (6):

$$\left[\begin{aligned}
\frac{\partial L}{\partial \theta} &= -i_1 \psi_f \sin \theta - i_2 \psi_f \sin \left(\theta - \frac{2}{3} \pi \right) \\
&\quad - i_3 \psi_f \sin \left(\theta + \frac{2}{3} \pi \right) \\
\frac{\partial L}{\partial \dot{\theta}} &= J_s \frac{d\theta}{dt} + J_b \frac{d\theta}{dt} \\
\frac{d}{dt} \left(\frac{\partial L}{\partial \dot{\theta}} \right) &= J_s \frac{d}{dt} \left(\frac{d\theta}{dt} \right) + J_b \frac{d}{dt} \left(\frac{d\theta}{dt} \right) \\
\frac{\partial E_r}{\partial \dot{\theta}} &= R_b \left(\frac{d\theta}{dt} \right)
\end{aligned} \right. \quad (12)$$

Bring the above formula into equation (2) to obtain the vibration displacement equation of the flexible manipulator in the system:

$$\begin{aligned}
\left[J_s + J_b \right] \frac{d}{dt} \left(\frac{ds}{dt} \right) &+ i_1 \psi_f \sin \theta + i_2 \psi_f \sin \left(\theta - \frac{2}{3} \pi \right) \\
&+ i_3 \psi_f \sin \left(\theta + \frac{2}{3} \pi \right) + R_b \left(\frac{d\theta}{dt} \right) = 0
\end{aligned} \quad (13)$$

Similarly, when the displacement of the flexible manipulator is selected as the research object in generalized coordinates, the following can be obtained:

$$\begin{aligned}
\left[\frac{m_s D^2 \pi}{4p} + m_b \right] \frac{d}{dt} \left(\frac{dS}{dt} \right) &- \left(\frac{2\pi}{P} \right) \left(\theta - \frac{2\pi S}{p} \right) K_b \\
&+ R_f \left(\frac{dS}{dt} \right) = 0
\end{aligned} \quad (14)$$

In summary, the global electromechanical coupling dynamic equations of the system can be obtained by combining equations (9), (10), (11), (13) and (14):

$$\begin{aligned}
u_1 &= L_1 \frac{di_1}{dt} + H_n \left(\frac{di_2}{dt} \right) + H_n \left(\frac{di_3}{dt} \right) \\
&\quad - \frac{d\theta}{dt} \psi_f \sin \theta + R_1 i_1 \\
u_2 &= L_2 \frac{di_2}{dt} + H_n \left(\frac{di_1}{dt} \right) + H_n \left(\frac{di_3}{dt} \right) \\
&\quad - \frac{d\theta}{dt} \psi_f \sin \left(\theta - \frac{2}{3} \pi \right) + R_2 i_2 \\
u_3 &= L_3 \frac{di_3}{dt} + H_n \left(\frac{di_1}{dt} \right) + H_n \left(\frac{di_2}{dt} \right) \\
&\quad - \frac{d\theta}{dt} \psi_f \sin \left(\theta + \frac{2}{3} \pi \right) + R_3 i_3 \\
\left[J_s + J_b \right] \frac{d}{dt} \left(\frac{dS}{dt} \right) &+ i_1 \psi_f \sin \theta + i_2 \psi_f \sin \left(\theta - \frac{2}{3} \pi \right) \\
&+ i_3 \psi_f \sin \left(\theta + \frac{2}{3} \pi \right) + \int_0^L \rho s \left(\frac{D}{2} + \frac{\partial w}{\partial t} \right)^2 \\
&+ R_b \left(\frac{d\theta}{dt} \right) = 0 \\
\left[\frac{m_s D^2 \pi}{4p} + m_b \right] \frac{d}{dt} \left(\frac{dS}{dt} \right) &- \left(\frac{2\pi}{P} \right) \left(\theta - \frac{2\pi S}{p} \right) K_b \\
&+ R_f \left(\frac{dS}{dt} \right) = 0
\end{aligned} \tag{15}$$

From the above formula, it can be concluded that there is a coupling phenomenon between the mechanical structure parameters of the AC permanent magnet servo motor such as current, and motor angle and the vibration displacement of the flexible operating arm. With the change

of input parameters of AC permanent magnet servo motor, the vibration displacement parameters of flexible manipulator also change, which has a certain impact on the operation accuracy of end effector. Therefore, the theoretical derivation of the global electromechanical coupling based on the above system has an important theoretical basis for exploring the vibration mechanism of the flexible arm, the optimal design of the mechanism and improving the positioning accuracy of the system.

III. Establishment of System Global Electromechanical Coupling Model and Design of Virtual Simulation Platform

1. Composition of Flexible Manipulator System Experiment Object

Considering that the global electromechanical coupling dynamic model of the above system is a set of nonlinear differential equations, it is difficult to obtain an accurate solution. Therefore, based on the determined global electromechanical coupling dynamic model of the system, a virtual simulation platform of the flexible manipulator system will be built with the help of MATLAB/Simulink for numerical example analysis. Before establishing the global electromechanical coupling model of flexible manipulator system and the experimental test and analysis of vibration characteristics, the parameters of each mechanical component are established first.

(1) In order to meet the characteristics of high strength and light weight of flexible manipulator. The experimental system uses epoxy fiber board as the flexible manipulator, which has greater stiffness and lighter weight than aluminum. The physical parameters of epoxy resin fiberboard are shown in table 2-1:

Table 2-1 Physical parameters of the flexible manipulator

Material	Length/mm	Width/mm	Thickness/mm	Density/ $kg.m^3$	Elastic modulus/Gpa	Poisson's ratio
Epoxy Resin	350	50	4	2030	25.24	0.30

(2) The flexible manipulator driving subsystem adopts the most widely used permanent magnet AC servo motor, its model is MHNJ042GIU, and the motor can detect the

operation of each driving motor by relying on its own encoder. Specific physical parameters are shown in table 2-2:

Table 2-2 Physical parameters of permanent magnet synchronous AC servo motor

Model	Rated power /W	Rated torque /N·m	Rated speed /r·min ⁻¹	Maximum speed /r·min ⁻¹	Rotor inertia /×E-0.4kg·m ²	Encoder specification
MHMJ042GIU	400	1.3	3000	5000	0.67	20 bit incremental

(3) The transmission system is the key component connecting the drive system and the execution system. In this experimental system, the ball screw pair produced by

Taiwan TBI company is used, and its main performance parameters are shown in table 2-3:

Table 2-3 Physical parameters of ball screw pair

Model TBI	External diameter/mm	Lead/mm	Nut diameter/mm	Nut length/mm	Dynamic load/kgf
SFS1610	15	10	28	47	839

Based on the determination of the parameters of the above parts, finally the RP flexible manipulator experimental platform is built as shown in Fig.4. The flexible operating arm is fixedly connected to the moving slider of the roller lead screw through bolts. Under the

action of the driving torque of AC permanent magnet synchronous motor 1 and 2, the roller lead screw and the moving slider can realize rotation and translation movement, and then drive the flexible operating arm fixed on the moving slider to complete the specified operation.

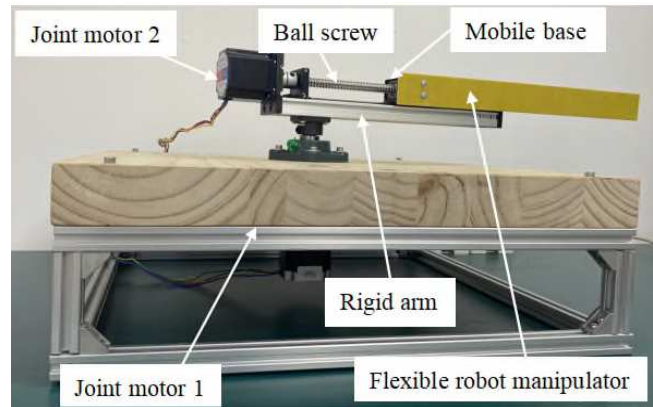


Figure 4 flexible manipulator experimental platform

2. Motion Characteristic under Electromechanical Coupling Effects

By solving the above equation (15), the output characteristics of the AC permanent magnet synchronous motor and the moving slider in the flexible manipulator system can be obtained, and then the output characteristics of the moving base can be taken as the input, so as to obtain the dynamic characteristics of the flexible manipulator in the form of electromechanical coupling. In order to achieve the above purpose, this paper will use the modeling method

of the combination of module connection and programming, and build the virtual simulation experimental platform of RP flexible manipulator with the help of MATLAB / Simulink, carry out dynamic simulation analysis on the coupling relationship in the mechanical structure, and study the motion speed characteristics between the driving motor and the moving slider base. The Simulink simulation model is shown in Fig.5:

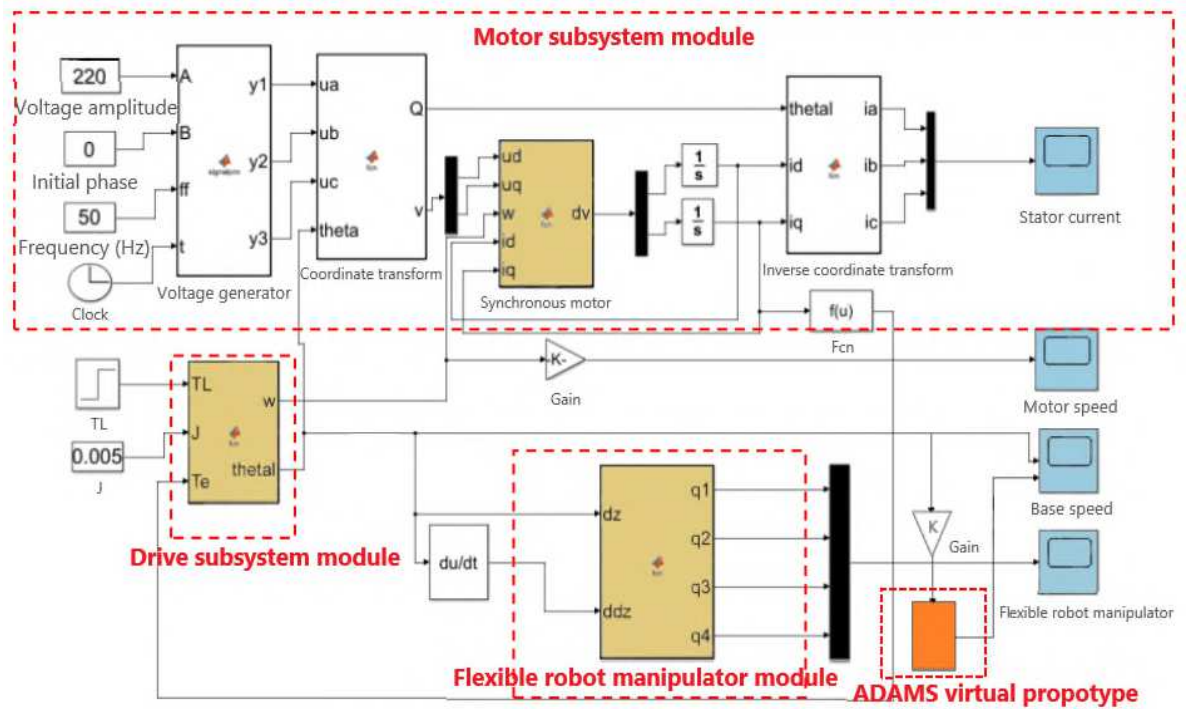


Figure 5 Simulink model of system global virtual simulation under Electromechanical Coupling

The specific process of the virtual simulation platform is as follows: firstly, the output speed and output torque of the drive motor are solved by the drive subsystem module, and then imported into the drive subsystem module to solve the speed and acceleration of the slider base, finally, the dynamic characteristics and output characteristics of the flexible manipulator in the form of electromagnetic torque direct coupling can be obtained by importing into the flexible manipulator subsystem module.

(1) Speed characteristics of drive motor

In order to study the speed characteristics of the driving motor, the frequency of the power supply is set as $f = 30\text{Hz}$, 40Hz and 50Hz respectively. According to the calculation formula of synchronous motor speed:

$$\gamma = \frac{60 f}{P} \quad (16)$$

The output speeds of permanent magnet synchronous motor can be calculated as 450r/min , 600r/min and 750r/min respectively. Where, f represents the stator voltage frequency of the permanent magnet synchronous motor, P represents the pole pairs of the permanent magnet synchronous motor and γ represents the output speed of the permanent magnet synchronous motor.

According to the Simulink dynamic coupling simulation model built above, when the three-phase voltage frequency of the motor is set as 30Hz , 40Hz and 50Hz respectively, the output speed curve of the synchronous motor can be obtained, as shown in Fig.6.

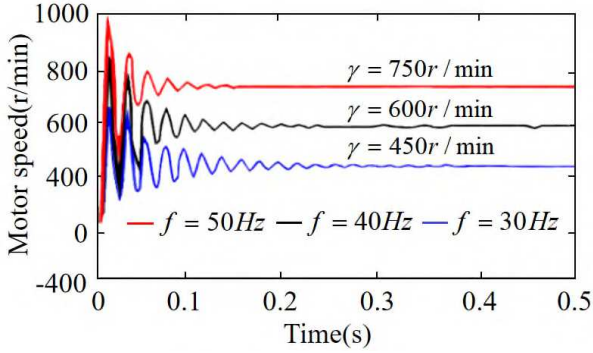


Figure 6 The output speed of AC permanent magnet motor

It can be seen from the figure that the output speed of the driving motor obtained by the virtual simulation model fluctuates obviously at the initial stage, and then gradually tends to 450r / min, 600r / min and 750r / min, which is the same as the results calculated by the theoretical calculation of the above formula (16), thus verifying the rationality of the virtual simulation model built in this section. At the same time, it can be seen that the electromechanical coupling in the system is mainly manifested in the oscillation of motor speed in the non-stationary stage of driving motor starting time.

(2) Study on characteristics of moving base

According to the above discussion, it can be seen that there are obvious fluctuations in the output characteristics of the drive motor, which is bound to be transmitted to the flexible arm through the transmission system, and then have a certain impact on the operation accuracy of the end effector. Based on the global electromechanical coupling Simulink model of the system established in Fig.5, similarly, the speed characteristic curve of the moving base under the set voltage and frequency can be obtained, as shown in Fig.7.

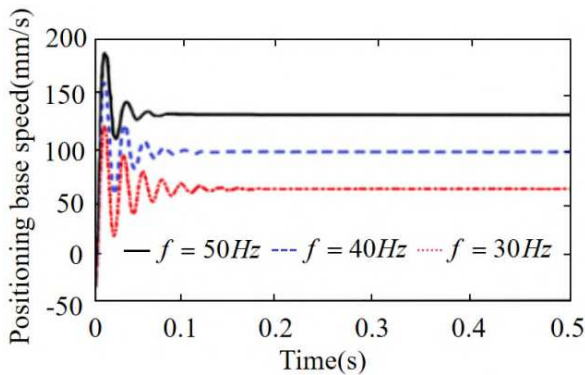
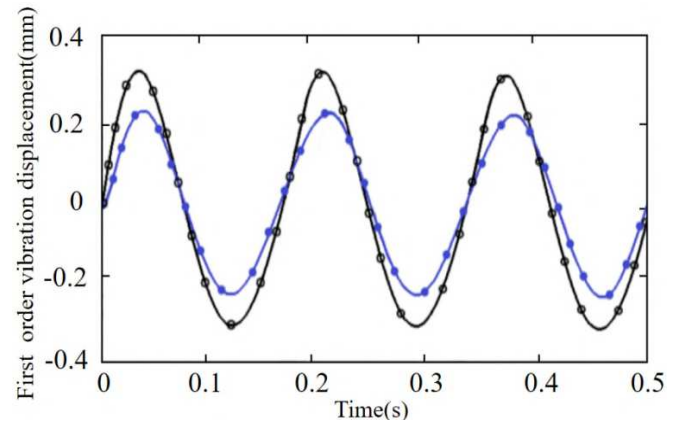


Figure 7 The velocity characteristic curve of moving base

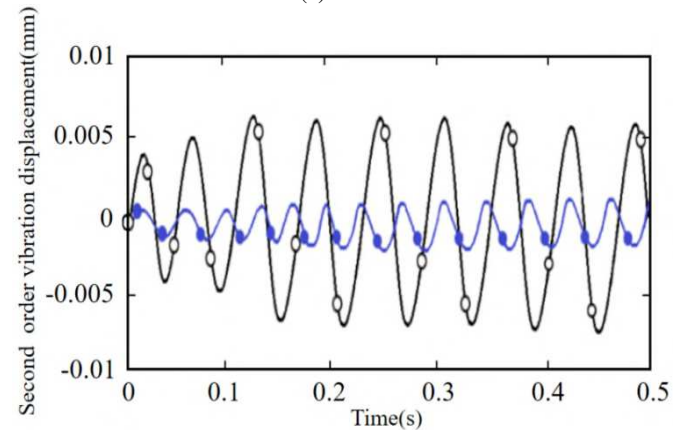
It can be seen from the figure that when the given voltage frequency is 30Hz, 40Hz and 50Hz, the speed of the corresponding moving base is 75mm / s, 100mm / s and 125mm / s respectively. It can also be seen that in the initial stage of the movement, there is an obvious fluctuation in the speed of the moving base due to the obvious fluctuation in the output speed of the driving motor, and then gradually tends to a stable state.

(3) Study on dynamic characteristics of flexible manipulator

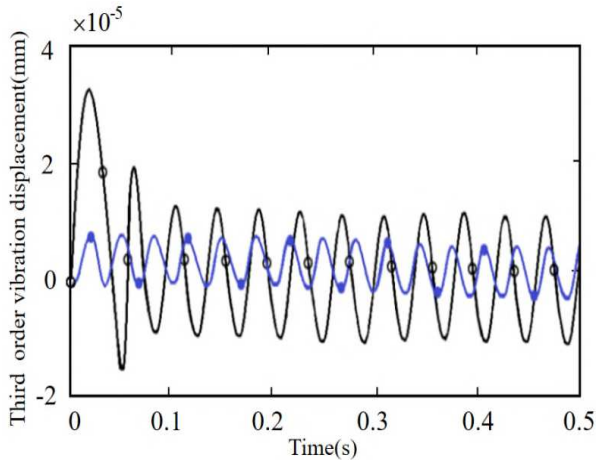
Also based on the virtual simulation platform of the global electromechanical coupling model of the system established in Fig.5, taking the three-phase stator voltage frequency of AC permanent magnet synchronous motor 30Hz as an example, the first three-order modal response displacement curves of the flexible operating arm considering the non-stationary in the start-up stage and not considering the non-stationary in the start-up stage are numerically simulated, as shown in Fig.8.



(a) First order



(b) Second order



(c) Third order

- ⊖ Considering the non-stationary process
- Not considering the non-stationary process

Figure 8 displacement curve of the first three modes of flexible manipulator under global electromechanical coupling effect and ideal start ($f=30\text{Hz}$)

As shown in Fig.8, the vibration displacement curves of the first three modes at the end of the flexible manipulator under the above two startup states are described respectively. It can be seen from the figure that the non-stationary process of permanent magnet motor in the starting stage has an obvious impact on the dynamic characteristics of flexible arm, that is, the increase of vibration displacement amplitude.

Also based on the virtual simulation platform of the global electromechanical coupling model of the system established in Fig.5, taking the three-phase stator voltage frequency of AC permanent magnet synchronous motor 30Hz as an example, the first three-order modal response displacement curves of the flexible operating arm considering the non-stationary in the start-up stage and not considering the non-stationary in the start-up stage are numerically simulated, as shown in Fig.8. order to further analyze the influence of the non-stationary process in the motor starting stage on the vibration at the end of the flexible arm, the voltage frequencies of the AC permanent magnet synchronous motor are set as 30Hz, 40Hz and 50Hz respectively. For different target speeds, the influence of the non-stationary transition process in the motor starting stage on the elastic vibration at the end of the flexible arm is considered, The vibration changes at the end of the flexible arm at different target speeds are obtained as shown in Fig.9.

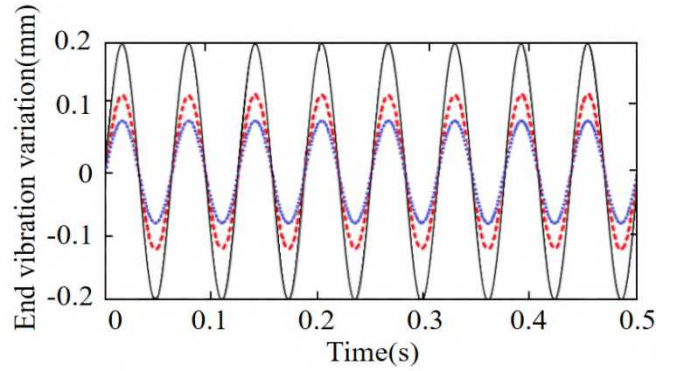


Figure 9 The variation of flexible arm end vibration at different target speeds

It can be seen from the above figure that the elastic vibration displacement amplitude at the end of the flexible arm is different at different speeds. The specific performance is that with the increase of the driving motor speed, the amplitude of the end vibration displacement also increases gradually, but the frequency remains basically unchanged, indicating that in the state of high-speed motion, the non-stationary process in the motor starting stage has a more significant impact on the dynamic characteristics of the flexible arm end. Therefore, in some occasions with high requirements for speed accuracy, it is more necessary to consider the influence of the non-stationary process of the motor in the starting stage.

According to the previous research and analysis, the output speed of the driving motor and the moving speed of the moving base have a certain degree of fluctuation under the electromechanical coupling of the system, which is bound to have a certain impact on the characteristics of the flexible arm. Therefore, based on MATLAB / Simulink and ADAMS / controls simulation software, a joint simulation model is established to further explore the vibration characteristics of flexible manipulator under electromechanical coupling.

By setting different power frequencies in Simulink, the flexible manipulator can be given different target speeds. According to the previous analysis, the system at this time has motion fluctuations. However, in Adams prototype experiment, the speed of the given moving base is ideal and constant, and there is no movement fluctuation. Thus, the comparison curve is obtained as shown in Fig.10.

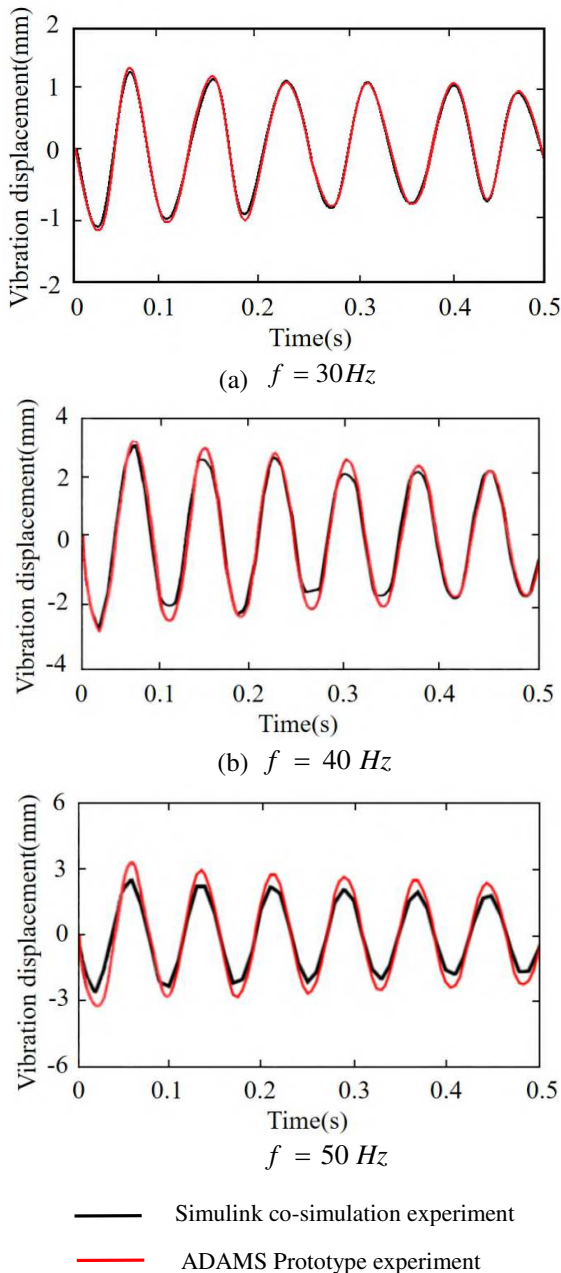


Figure 10 Comparison curve between Simulink co-simulation experiment and ADAMS prototype

As can be seen from the experimental results in the figure above, the mechanical and electrical coupling condition and the non-coupling condition have the same trend, but the response amplitude is larger. With the increasing speed of the moving frame, the vibration displacement of the flexible manipulator in the two cases is more and more obvious. It is further verified that the non-stationary process in the motor start-up stage has a more significant effect on the dynamic characteristics of the flexible arm.

IV. Conclusions

Taking the electromechanical coupling between RP flexible robot systems as the research object, the influence law of coupling effect on the dynamic characteristics of flexible arm is analyzed based on MATLAB, the influence mechanism is revealed, and the following conclusions are obtained:

(1) Considering the coupling between electromagnetic system and mechanical system, a global electromechanical coupling model is established; and the dynamic equation of mechanical structure is derived by using the electromechanical analysis dynamic method.

(2) The virtual simulation platform is constructed based on MATLAB/Simulink, the output speed characteristics of the driving end and the motion characteristics of the moving base are analyzed, and the vibration law of the flexible arm under electromechanical coupling is revealed.

(3) It is found that in the state of high-speed motion, the non-stationary process in the starting stage of the motor has a more significant impact on the dynamic characteristics of the end of the flexible arm. In some occasions with high requirements for speed accuracy, the impact of the non-stationary process in the starting stage of the motor should be considered.

Through the electromechanical coupling analysis between the systems, it provides a theoretical basis for the study of parametric vibration characteristics and elastic vibration control design of flexible arm.

REFERENCES

- [1] Shuxin Wang, Jurong Shi, et al. Review on modeling theory and control method of flexible manipulator[J]. Robotics,2002,24(1):86-91+96.
- [2] Liu Y F, Li W, Yang X F, et al. Coupled dynamic model and vibration responses characteristic of a motor-driven flexible manipulator system [J]. Mechanical Sciences, 2015, 6(2): 235-244.
- [3] Qiu Z C. Adaptive nonlinear vibration control of a Cartesian flexible manipulator driven by a ballscrew mechanism[J]. Mechanical Systems and Signal Processing, 2012, 30: 248-266.
- [4] Dwivedy S.K., Eberhard P. Dynamic analysis of flexible manipulators, a literature review[J]. Mechanism & Machine Theory, 2006, 41(41): 749-777.

- [5] Ostring M, Gunnarsson S, Norrlof M. Closed-loop identification of an industrial robot containing flexibilities [J]. *Control Engineering Practice*, 2003, 11(3): 291-300.
- [6] Lihong Lin, Xiaohan Chen, Chaoqun Zhou, et al. Electromechanical coupling modeling and simulation analysis of precision transmission system [J]. *Journal of Chongqing University (Natural Science Edition)*, 2007, 30(11): 14-18.
- [7] Bingheng Lu, Wanhua Zhao, et al. Electromechanical coupling of feed system under high speed and high acceleration [J]. *Journal of Mechanical Engineering*, 2013, 49(6): 2-11.
- [8] Zhicheng Qiu, Mingli Shi, Bin Wang, et al. Genetic algorithm based active vibration control for a moving flexible smart beam driven by a pneumatic rod cylinder [J]. *Journal of Sound and Vibration*, 2012, 331(10): 2233-2256.
- [9] Qiu Z C. Adaptive nonlinear vibration control of a Cartesian flexible manipulator driven by a ballscrew mechanism [J]. *Mechanical Systems and Signal Processing*, 2012, 30: 248-266.
- [10] Barun Pratihier, Santosha Kumar Dwivedy. Non-linear dynamics of a flexible single link Cartesian manipulator [J]. *International Journal of Non-Linear Mechanics*, 2007, 42(9): 1062-1073.
- [11] Jiajun Qiu. Nonlinear vibration of electromechanical coupled dynamical system [M]. Science Press, 1996.
- [12] Jiajun Qiu. Research progress of electromechanical coupling dynamics [J]. *Mechanical progress*, 1998, 28(04): 453-460.
- [13] Meng J, Chen X A et al. Electromechanical coupling dynamic modeling of high speed motorized spindle motor spindle system [J]. *Journal of Mechanical Engineering*, 2007, 43(12): 160-165.
- [14] Ailun Wang, Ju Zhong. Research on global coupling modeling method and Simulation of complex electromechanical system [J]. *Journal of Mechanical Engineering*, 2003, 39(04): 1-5.
- [15] Subudhi B, Morris A S. Dynamic modelling, simulation and control of a manipulator with flexible links and joints [J]. *Robotics and Autonomous Systems*, 2002, 41(4): 257-270.
- [16] Tang H P, Zhong J. A global modeling method for complex electromechanical systems [J]. *Journal of Central South University (Natural Science Edition)*, 2002, 33(5): 522-525.
- [17] Felix J.L.P., Balthazar J.M. Comments on a nonlinear and nonideal electromechanical damping vibration absorber, Sommerfeld effect and energy transfer [J]. *Nonlinear Dynamics*, 2009, 55(1-2): 1-11.
- [18] Dwivedy S K, Kar R C. Simultaneous combination and 1:3:5 internal resonances in a parametrically excited beam-mass system [J]. *International Journal of Non-Linear Mechanics*, 2003, 38(4): 585-596.
- [19] Ju Jinyong, Li Wei, Wang Yuqiao, Fan Mengbao, Yang Xuefeng. Dynamics and nonlinear feedback control for torsional vibration bifurcation in main transmission system of scraper conveyor direct driven by high-power PMSM [J]. *Nonlinear dynamics*.
- [20] Ju Jinyong, Li Wei, Yang Xuefeng, Wang Yuqiao, Liu Yufei. Electromechanical coupling vibration characteristics of an AC servomotor-driven translational flexible manipulator [J]. *International Journal of Advanced Robotic Systems*, 2016, 13(6): p. 1-10.
- [21] Liu Y F, Li W, Yang X F, et al. Coupled dynamic model and vibration responses characteristic of a motor-driven flexible manipulator system [J]. *Mechanical Sciences*, 2015, 6(2): 235-244.
- [22] Wuling Hao, Wei Zhang. Nonlinear dynamics of thin plates under combined parametric and external excitation [J]. *Journal of dynamics and control*, 2014, 12 (2) : 139-146.
- [23] Yao M H, Zhang W. Multi-pulse chaotic motions of high-dimension nonlinear system for a laminated composite piezoelectric rectangular plate [J]. *Meccanica*, 2014, 49(2): 365-392.
- [24] Li S B, Zhang W. Global bifurcations and multi-pulse chaotic dynamics of rectangular thin plate with one-to-one internal resonance [J]. *Applied Mathematics and Mechanics*, 2012, 33(9): 1115-1128.
- [25] Guo X Y, Zhang W, Yao M H. Multi-pulse orbits and chaotic dynamics of a composite laminated rectangular plate [J]. *Acta Mechanica Solida Sinica*, 2011, 24(5): 383-398.
- [26] Wei K X, Zhang W M, Xia P, Liu Y C. Nonlinear dynamics of an electrorheological sandwich beam with rotary oscillation [J]. *Journal of Applied Mathematics*, 2012, vol. 2012, Article ID 659872, 1-17.
- [27] Lou J Q. Research on integrated control of trajectory tracking and vibration suppression of space flexible manipulator system based on piezoelectric actuator [D]. Zhejiang University, 2013.
- [28] S S Ge, T H Lee, J Q Gong. A robust distributed controller of a single-link SCARA/Cartesian smart materials robot [J]. *Mechatronics*, 1999, 9: 65-93.
- [29] Liou F W, Erdman A G, Lin C S. Dynamic analysis of a motor-gear-mechanism system [J]. *Mechanism and Machine Theory*, 1991, 26(3): 239-252.
- [30] Smaili A, Koppapu M, Sannah M. Elastodynamic response of a dc motor driven flexible mechanism system with compliant drive train components during start-up [J]. *Mechanism and Machine Theory*, 1996, 31(5): 659-672.
- [31] Korayem M.H., Bamdad M., Tourajizadeh H., et al. Experimental results for the flexible joint cable-suspended manipulator of ICa Sbot [J]. *Robotica*, 2013, 31(31): 887-904.
- [32] Korayem Moharam Habibnejad, Rahimi H. N., Nikoobin, A. Mathematical modeling and trajectory planning of mobile

manipulators with flexible links and joints[J].Applied Mathematical Modeling, 2012,36(7): 3223-3238.

- [33] Xuedan Wang, Jianguo Jiang. Modeling and control of nonlinear coupling vibration of motor drive system[J]. Journal of coal, 2004, 29(5): 622-625.
- [34] Liu Yufei, Li Wei, Wang Yuqiao, et al. Dynamic model and vibration power flow of a rigid-flexible coupling and harmonic-disturbance exciting system for flexible robotic manipulator with elastic joints[J]. Shock and Vibration, 2015 vol. 2015, Article ID 541057, 1-10.
- [35] Liu Yufei, Li Wei, Yang Xuefeng, et al. Study on coupling vibration characteristics of flexible manipulator under disturbance excitation of linear positioning platform[J]. Shock and Vibration, 2015, 34(15): 1-6.
- [36] Liu S., Li X., Zhao S., et al. Bifurcation and chaos analysis of a nonlinear electromechanical coupling transmission system driven by AC asynchronous motor[J]. International Journal of Applied Electromagnetics & Mechanics, 2015, 47(3): 705-717.



Zhang wenhui was born in 1980. He received his Ph.D. degree in engineering field from Harbin Institute of Technology, Harbin, PR China, 2011. He is now a professor at School of electronic engineering, Nanjing Xiaozhuang University, Nanjing, PR China. His research interests include study on dynamic characteristics of flexible robots, robot control technology, etc. In this study, he proposed the general research scheme of dynamic characteristics of flexible robot,

gave new ideas and methods, and determined the research objectives.